PNAS RESEARCH ARTICLE | NEUROSCIENCE OPEN ACCESS

Goal discrimination in hippocampal nonplace cells when place information is ambiguous

Lu Zhang[a], Stephanie M. Prince[a,b], Abigail L. Paulson[a], and Annabelle C. Singer[a,1]

Edited by Nancy Kopell, Boston University, Boston, MA; received April 18, 2021; accepted January 30, 2022

Memory-guided navigation relies on hippocampal neurons, like place cells, that encode features of the environment. However, little is known about hippocampal place codes when spatial cues provide ambiguous information about finding goals. Nonplace cells, pyramidal cells that fire without strong spatial modulation in an environment, may be well-suited to carry task-relevant information when spatial information is ambiguous. We find that when spatial cues and goal information are conflicting, nonplace cell firing distinguishes between ambiguous spatial cues. On correct trials nonplace cells had higher firing rates and altered gamma-phase modulation at task-relevant cues than on incorrect trials, while place cells showed no such differences. Finally, this goal discrimination in nonplace cells is absent in a mouse model of Alzheimer's disease that has memory impairment. Our findings show that nonplace cells differentiate ambiguous goal information that place cells do not, revealing a special contribution to coding by these nonplace cells.

hippocampus | navigation | place cells | nonplace cells | decoding

Significance

Goal-directed spatial navigation has been found to rely on hippocampal neurons that are spatially modulated. We show that "nonplace" cells without significant spatial modulation play a role in discriminating goals when environmental cues for goals are ambiguous. This nonplace cell activity is performance-dependent and is modulated by gamma oscillations. Finally, nonplace cell goal discrimination coding fails in a mouse model of Alzheimer's disease (AD). Together, these results show that nonplace cell firing can signal unique task-relevant information when spatial information is ambiguous; these signals depend on performance and are absent in a mouse model of AD.

Memory-guided navigation requires integrating information about position with task demands, such as how to reach a goal (1–3). While the hippocampus is central to representing spatial information (4, 5), less is known about hippocampal roles when spatial and task-relevant nonspatial information is conflicting, for example when spatial information is misleading about goals. Hippocampal place cells, which represent an animal's spatial position in an environment, are thought to be central to goal-directed navigation (6–13). Place cells' firing fields have been shown to cluster around goal locations (14–16), and small subpopulations of hippocampal cells (less than 6%) have been found to represent reward locations (17, 18). However, coding for goal information by place cells presents specific challenges in that a pure goal code would lead to all cells firing at the goal instead of tiling the environment as place cells typically do (9, 19). This conflict can be solved in two ways: Either hippocampal cells conjunctively encode both place and goal information (20) or goal information is conveyed in other brain regions (21). Several studies have reported evidence of conjunctive hippocampal codes within individual neurons, such as conjunctive item-place cells representing both salient items (what) and place (where) (22), as well as hybrid place cells that integrate both place and reward information (18). Studies have also shown that some cells code for distance to goals (23–25). In most reports conjunctive coding cells are still highly spatially modulated with clear spatial receptive fields. While these studies indicate that hippocampal cells can code for both goal and place information, such place-reward conjunctive coding would fail when spatial information about reward is ambiguous. Thus, it remains unclear how spatially modulated cells accurately guide navigation and how place and goal information is encoded when similar spatial cues indicate both goal and nongoal locations. Recent evidence has shown that cells that are not significantly spatially modulated, or nonplace cells, contribute to population-level spatial coding in hippocampus (26, 27). These findings lead to questions about the role of nonplace cells in coding for task-relevant features during goal-directed navigation when spatial information is ambiguous.

Spike timing of hippocampal cells relative to oscillatory brain activity is central to memory-guided navigation performance. Oscillatory activity differs between correct and incorrect trials during navigation, and gamma oscillations (30 to 150 Hz) in particular play a role in navigation performance (28–35). Studies have shown that slow [30 to 50 Hz (29)] or medium (65 to 120 Hz, reported as high gamma in ref. 28 and referred to here as medium gamma) gamma oscillations increased prior to correct trials in an avoidance task or alternation task, respectively. During gamma, the firing of many single neurons is coordinated such that many cells fire together at a preferred phase of the oscillation (33, 34, 36–40). Coordinated spike timing is thought to amplify spatial codes by driving neurons to fire together in short time windows such

Author affiliations: [a]Coulter Department of Biomedical Engineering, Georgia Institute of Technology, Atlanta, GA 30332; and [b]Neuroscience Graduate Program, Graduate Division of Biological and Biomedical Sciences, Emory University, Atlanta, GA 30322

Author contributions: L.Z., S.M.P., A.L.P., and A.C.S. designed research; S.M.P., A.L.P., and A.C.S. performed research; L.Z. and A.C.S. contributed new reagents/analytic tools; L.Z., S.M.P., A.L.P., and A.C.S. analyzed data; and L.Z., S.M.P., A.L.P., and A.C.S. wrote the paper.

The authors declare no competing interest.

This article is a PNAS Direct Submission.

[1]To whom correspondence may be addressed. Email: asinger@gatech.edu.

This article contains supporting information online at http://www.pnas.org/lookup/suppl/doi:10.1073/pnas.2107337119/-/DCSupplemental.

Published March 7, 2022.

that the coordinated cells more effectively drive downstream neurons (28, 29). Given that nonplace cells contribute to hippocampal representations of an environment, the spike timing of this subpopulation during gamma oscillations may play a unique role in navigation performance as well. While gamma modulation of hippocampal pyramidal cells has been widely reported (38, 41–43), little is known about how gamma modulation of nonplace cells in particular relates to navigation performance.

Here we evaluate the role of nonplace cells in processing goal information in a goal-guided spatial task when spatial cues are ambiguous. We hypothesized that while both place and nonplace cells represent information like distance to goals, nonplace cells would better represent nonspatial information like disambiguating true and false goal information because these cells do not code significant place information. To test this hypothesis, we designed a goal-directed virtual reality (VR) spatial navigation task in which spatial cues provide ambiguous information about the goal, e.g., the same cue indicates a false or true goal. Our repeated cue design allowed us to explicitly test differences in coding during the correct and incorrect trial performance when spatial information was ambiguous. We used a VR task, as animals navigating in VR have previously been shown to have strong distance-to-goal coding in the hippocampus (25). Nonplace cells were identified as those that did not have significant spatial information in the track. We examined nonplace cell firing patterns relative to cues, spatial position, and goals and we assessed firing rates as well as spike timing relative to theta and gamma oscillations. We found firing of nonplace cells better discriminated between false and true goals at both the single-cell level and the population level. We then determined if nonplace cell firing was modulated by task performance. Nonplace cells, but not place cells, significantly differed between correct and incorrect trials in both their firing rates and phase modulation by gamma at the false goal. Finally, in a mouse model of Alzheimer's disease (AD) that has memory impairment, nonplace cells failed to discriminate between false and true goals. Our findings indicate that nonplace cells are goal-discriminating. These goal-discriminating cells carry key task information that disambiguates vague spatial cues and is not present in place cells. This type of goal disambiguating coding fails in a mouse model of AD.

Results

Animals Perform VR Navigation Task with False Goal Cues. To assess how nonplace cells in the hippocampus contribute to neural codes for place, cues, and goals, we designed a VR task to assess neural responses as a function of visual cues, distance to rewards, and global position in the environment (*SI Appendix,* Fig. S1*A*). In a VR task without self-motion cues we expected diverse codes, such as distance codes, to be more prominent based on prior work, allowing us to assess both place and distance to goal coding (25, 44). In this task mice ran around a ring-shaped track and licked in two goal zones. The mouse performed a correct trial when it licked in the goal zone, which then triggered reward delivery (see *SI Appendix, Supplementary Methods*). The two goal zones had distinct wall patterns leading up to them, but the pattern indicating the goal zone was repeated twice such that the same cue was in both a rewarding and nonrewarding position. The first appearance of the wall pattern that was identical to the goal zone served as a type of "false goal zone." Thus, the reward location could not be distinguished by the wall cues alone but by the sequence of cues passed on the way to the reward zone, the distance traversed, and by distal cues. Animals were not penalized for slowing down and licking at the false goal zone, but this behavior delayed reaching the correct reward location. Indeed, mice licked at the false goal zone more than other nonreward zones ($P = 0.010$, $t_{16} = 2.900$ using paired t test with sessions, $P = 0.024$ using paired hierarchical bootstrap test to control for the different session numbers across individual mice; $q < 0.1$, false discovery rate [FDR] correction of 54 comparisons; *SI Appendix,* Table S4 and see *SI Appendix, Statistics* for details). They licked much less at the false goal zone than at the true goal zone [*SI Appendix,* Fig. S1 *B* and *C*; $P = 3.15\text{e-}6$, $t_{16} = 6.971$ using paired t test, $P = 0$ using paired hierarchical bootstrap test; $q < 0.1$, FDR correction of 54 comparisons; $P = 0$, $F_{2,68}$ (location) $= 107.652$; $P = 0.330$, $F_{1,34}$ (genotype) $= 0.979$; $P = 0.062$, $F_{2,68}$ (location × genotype) $= 2.892$ using two-way mixed ANOVA for lick rate]. In wild-type (WT) mice, speed at the false goal zone did not differ significantly from other nonreward zones, although there was a trend of some slowing at the false goal zone [$P = 0.114$, $t_{16} = -1.670$ using paired t test, $P = 0.091$ using paired hierarchical bootstrap test; $P = 1.52\text{e-}14$, $F_{2,68}$ (location) $= 52.677$; $P = 0.101$, $F_{1,34}$ (genotype) $= 2.850$; $P = 4.32\text{e-}4$, $F_{2,68}$ (location × genotype) $= 8.702$ using two-way mixed ANOVA for speed].

Nonplace Cells Discriminate between Real and False Goals Better than Place Cells. We hypothesized that while both place and nonplace cells represent information about current place and distance to goals, nonplace cells would better disambiguate true and false goal zones. We identified nonplace cells that were not significantly spatially modulated and place cells that were significantly spatially modulated from neurons recorded from hippocampal CA1. While place cells had spatial information content in the 95th percentile or above compared to shuffled spike train data, nonplace cells were identified by their lack of significant spatial information (threshold of $P = 0.05$, permutation test; see *SI Appendix, Supplementary Methods* for details). Many of the place cells recorded had multiple place fields (Fig. 1 *A* and *B*, *Left*). These results are similar to previous reports of multiple place fields per cell in large environments (45), in environments with similar, repeated features (46), or in VR environments with distance-coding cells (25). To determine whether cells discriminated between false and true goals, we compared firing between the part of the track leading up to the false goal zone (false goal similarity, first and third quarters of the track; Fig. 1*C*, *Middle*) or the true goal (true goal similarity, second and fourth quarters of the track; Fig. 1*C*, *Right*). We defined a goal discrimination index (GDI) which ranged from −1 to 1 to quantify how cells discriminated true and false goal zones (see *SI Appendix, Supplementary Methods* for details). Positive values of GDI represented higher firing similarity between the two segments approaching the true goal compared to the two segments approaching the false goal, where values approaching the maximal value of 1 represented a cell that fired very similarly leading up to both true goals but very differently leading up the false goals. We controlled for the effects of speed and licking on GDI using partial correlation and considering both speed and licking as covariates to determine if these factors explain observed differences in firing (*SI Appendix,* Figs. S2 and S3*A*; see *SI Appendix, Supplementary Methods* for details). We found the effects observed remain in both the raw correlation, in which speed and licking are not considered (*SI Appendix,* Fig. S3*B*), and partial correlation, in which the effects of speed and licking are regressed out, between true and

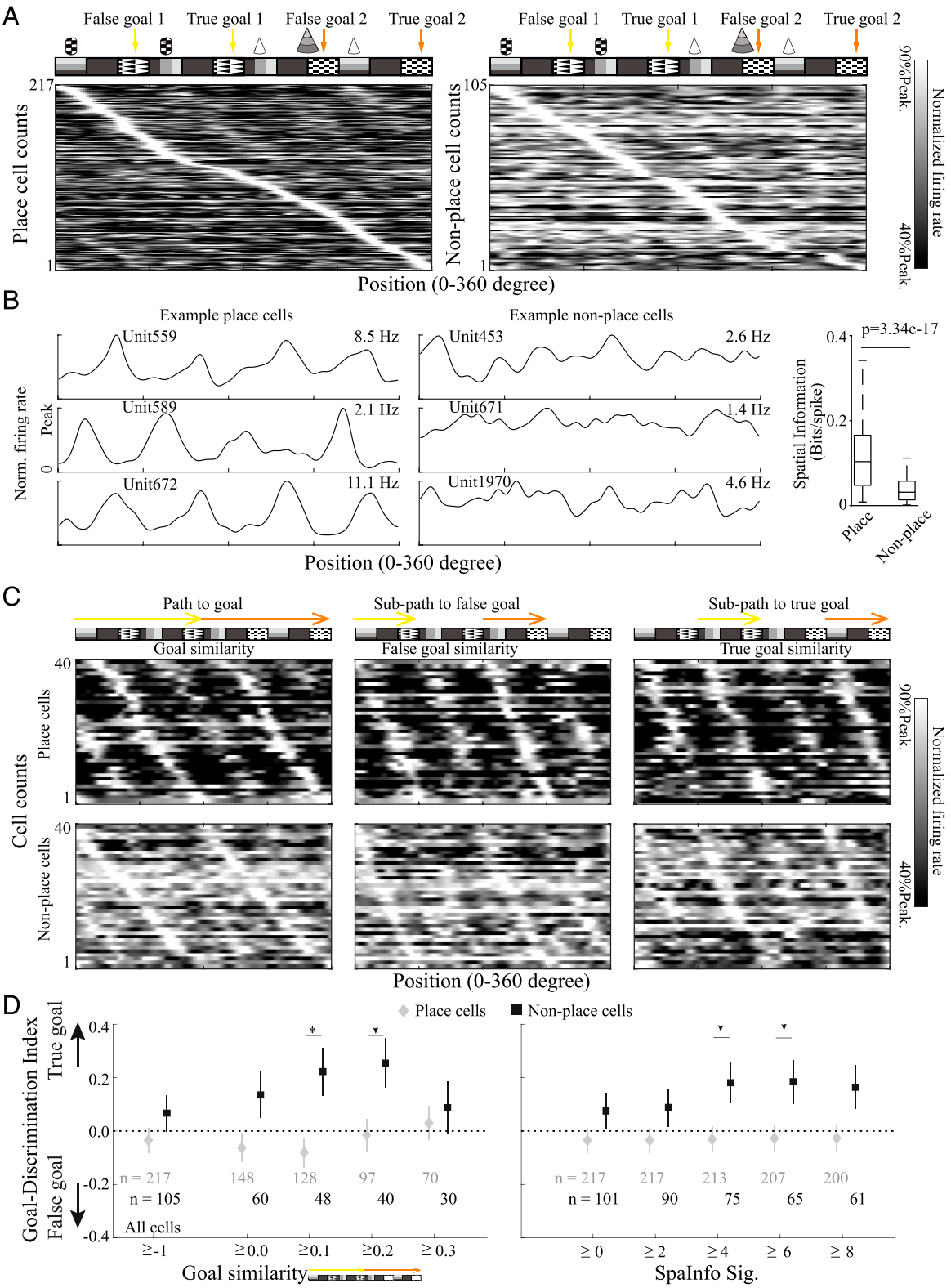

Fig. 1. Goal discriminability in CA1 pyramidal cells in WT mice. (*A*) Schematic of repeated wall patterns in the environment (*Top*). Normalized firing rates as a function of position for all place (*Left, n* = 217) and nonplace pyramidal (*Right, n* = 105) cells organized by its peak firing position. (*B*) Firing rate as a function of position for three place (*Left*) and three nonplace (*Center*) cells. The peak firing rate is shown at the top right of each panel for each cell. Distributions of spatial information of place cells and nonplace cells (*Right, P* = 3.34e-17, Wilcoxon rank-sum test). (*C*) Normalized firing rates for 40 place cells (*Top*) and nonplace cells (*Bottom*) with the highest similarity scores were organized by peak firing position. Three similarity scores (correlation coefficients) were computed between segments of the track (indicated with yellow and orange arrows) in three different ways: goal similarity score, false goal similarity score, and true goal similarity score, from left to right, respectively (see *SI Appendix, Supplementary Methods*). (*D*) Comparisons of GDI, defined as (True goal similarity − False goal similarity)/(|True goal similarity|+|False goal similarity|) (see *SI Appendix, Supplementary Methods* for details) between place cells and nonplace cells were made with two different inclusion criteria based on the goal similarity (*Left*) and spatial information significance (SpaInfo Sig., *Right*), respectively. Asterisk indicates significant differences (unpaired *t* test, q < 0.1, FDR correction of 20 comparisons = 10 groups × 2 genotypes); black arrowhead denotes less-strict statistics (*P* < 0.05, unpaired *t* test with no FDR correction).

false goal zones (*SI Appendix*, Fig. S3*C*). We then assessed GDI as a function of spatial coding (spatial information significance; see *SI Appendix, Supplementary Methods*) and distance to goal coding (goal similarity; see *SI Appendix, Supplementary Methods*) for individual place and nonplace cells.

We found nonplace cells discriminated between true and false goal zones while place cells did not. The GDIs of place cells, when grouped together, were close to zero (Fig. 1*D*, *Left*, all cells), consistent with place cells representing multiple parts of the track without a clear preference for the true or false goal (*SI Appendix*, Fig. S4*A*, *Top*, first column; $P = 0.614$, $t_{216} = 0.505$, paired t test). Nonplace cells had a trend of positive GDIs, although it was not significantly different from place cells [Fig. 1*D*, *Left*; all cells, $P = 0.221$, $t_{320} = -1.226$ unpaired t test for GDI; *SI Appendix*, Fig. S4*A*, *Top*, first column; $P = 0.097$, $F_{1,320}$ (cell type × similarity type) = 2.768, two-way mixed ANOVA for all cells]. We then segregated the population based on cells' goal similarity or spatial coding. Goal similarity measured how similarly the cell fired on paths to the two true goals (measured by correlating firing across the two paths to the true goals) in contrast to GDI, which measured how differently the cell fired on the subpaths to the true goals and false goals. For cells with higher goal similarity, nonplace cells had positive GDIs, significantly higher than those of place cells (Fig. 1*D* *Left*; $P = 0.005$, $t_{174} = -2.866$ unpaired t test of GDI for subgroup of cells with goal similarity ≥0.1; q < 0.1, FDR correction for 20 comparisons). Consistent with positive GDIs, we observed nonplace cells had significantly more similar firing at the true goal than the false goal, in contrast to place cells which showed no clear differences [*SI Appendix*, Fig. S4*A*, *Top*, third column; $P = 0.013$, $F_{1,174}$ (cell type × similarity type) = 6.367, two-way mixed ANOVA for goal similarity ≥0.1]. Both place and nonplace cells had similar GDIs close to zero for cells with very high goal similarity (Fig. 1*D*, *Left*; goal similarity ≥0.3), because similar firing across both false and true goals will lead to extremely high goal similarity (*SI Appendix*, Fig. S4*A*, *Top*). Thus, among cells that code distance to goal information, nonplace cells show consistent firing patterns approaching the true goal zone, and their firing discriminated between the true and false goals.

We then tested whether stronger coding for global position influenced goal discrimination in nonplace and place cells by examining GDI across different thresholds for spatial information significance. We found nonplace cells, but not place cells, discriminated between true and false goals even when these cells had high spatial information significance [Fig. 1*D*, *Right*; $P = 0.023$, $t_{286} = -2.280$ unpaired t test of GDI for SpaInfoSig. ≥ 4; q > 0.1, FDR correction for 20 comparisons; *SI Appendix*, Fig. S4*B*, *Top*, third column; $P = 0.003$, $F_{1,286}$ (cell type × similarity type) = 9.146, two-way mixed ANOVA for SpaInfoSig. ≥4]. In addition, the goal-discriminating properties of nonplace cells were not explained by the firing of high spatially tuned low-firing cells (*SI Appendix*, Fig. S5). Changes in neural activity at the false goal zone could indicate reward expectation or reward prediction error. To investigate this, we measured neural activity around the time of each lick and compared licks in the false goal zone (P3), which never led to reward, and licks in the true goal zone (P6) preceding reward delivery. We found very few cells were significantly modulated before or after licks (*SI Appendix*, Fig. S6). These results show that place cells code for a range of positions but do not discriminate between true and false goals with the same cues. In contrast, nonplace cells fire in consistent patterns for true goals and their firing activity discriminates between true and false goals. Thus, nonplace cell firing discriminates between similar cues when task-relevant information is different.

Nonplace Cells Improve Task-Relevant Codes Including Position, Distance to Goals, and False Goal Discrimination. We next determined nonplace cells' contributions to population-level representations of the environment to test the hypothesis that nonplace cell hippocampal firing improves coding of task-relevant information, like place and goals. We used a Bayesian decoder to assess how all simultaneously recorded cells represented information about the environment as the animal traversed the track (see *SI Appendix, Supplementary Methods*) relative to chance levels (47–50), where chance is defined as all positions being equally represented. We found populations of cells decoded the animals' current position significantly above chances levels ($P = 2.46e\text{-}4$, $t_5 = 9.270$, one-sample t test, q < 0.1, FDR correction of eight comparisons) while other positions were generally decoded below chance levels ($P = 2.46e\text{-}5$, $t_5 = -9.270$, one-sample t test, q < 0.1, FDR correction of eight chance level comparisons), as expected based on many prior studies (Fig. 2*A*, *Left*) (48, 49, 51). We then determined how place and nonplace cells contributed to this decoding by excluding a subset of place or nonplace cells and recomputing decoded position (Fig. 2 *A* and *C*, determined by excluding 30% of pyramidal cells recorded; see *SI Appendix, Supplementary Methods*). Only a subset of place or nonplace cells were excluded to ensure each condition was reduced by the same number of cells and changes in decoding accuracy could not be explained by the number of included cells. Generally, we would expect decoding accuracy of the current position to be worse when excluding neurons if those neurons provide information about position. Comparing the exclusion of the same number of place or nonplace cells allowed us to directly contrast the contributions of these different cells. When nonplace cells were excluded, decoding probability of current position was significantly worse than when all cells were included ($P = 0.006$, $t_5 = 4.610$, paired t test, q < 0.1, FDR correction of six comparisons) but still higher than that when place cells were excluded [Fig. 2*B*; $P = 0.007$, $t_5 = -4.345$, paired t test, q < 0.1, FDR correction of six comparisons; $P = 1.36e\text{-}4$, $F_{2,10}$ (cell type) = 24.672, one-way repeated measure ANOVA]. These results show that nonplace cells contribute to accurate decoding of the current position, although not as much as place cells.

While population firing primarily encoded the animal's current position, the population activity also showed some decoding of related positions, such as locations with the same distance to the goal. To determine how nonplace cells and place cells contribute to coding of this task-related information, we then investigated decoding of the distance to goal by collapsing both halves of the track together for our analyses (Fig. 2*D*). Overall, decoding current distance to the goal regardless of path (e.g., the first or second half of the track) was significantly higher than chance ($P = 4.89e\text{-}4$, $t_5 = 8.015$, one-sample t test, q < 0.1, FDR correction of eight comparisons) but lower than coding for global spatial position ($P = 0.041$, $t_5 = 2.737$, paired t test, q < 0.1 FDR correction of eight comparisons), e.g., position along specific paths. In agreement with place cells' well-studied role in coding current position, excluding place cells reduced the probability of identifying the current location (Fig. 2*E*), and this decrease was not significantly different between the goal zone (−13.9% ± 8.5%, mean ± SD) and other zones (−7.4% ± 3.3%; $P = 0.068$, $t_5 = 2.319$, paired t test). Excluding place cells had similar effects on decoding accuracy of the current position at both the reward zone and other zones ($P = 0.284$, $t_5 = -1.199$, paired t test). Excluding either place or nonplace cells led to poorer decoding of

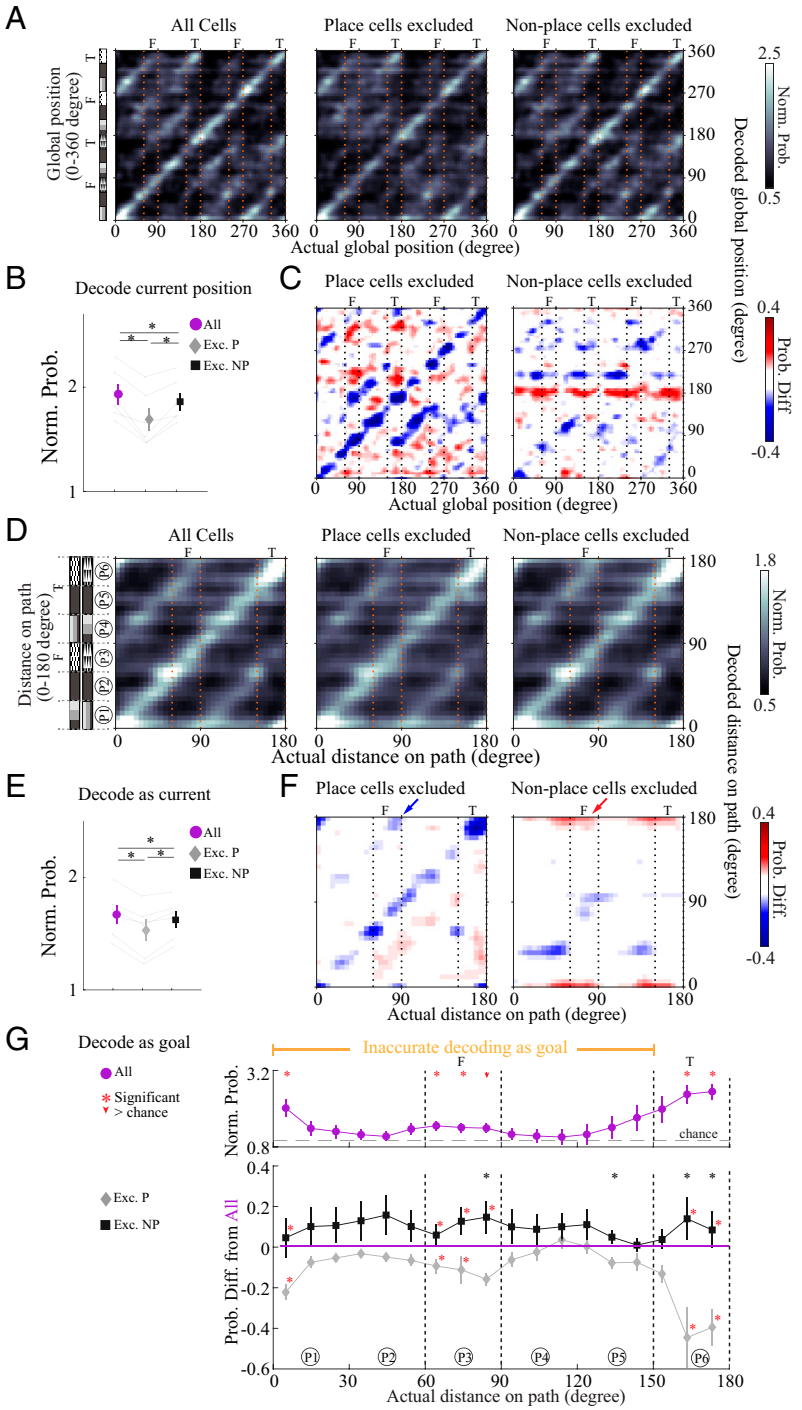

Fig. 2. Nonplace cells improve global position and distance to reward coding and enhance discrimination of false from true goal zone. (*A*) Heat map of normalized probability of decoding each position in the track as a function of actual position in the track for all cells (*Left*), with a subset of place cells excluded (*Center*), and with a subset of nonplace cells excluded (*Right*) averaged over recording sessions. Normalized probability of 1 indicates chance levels. ($n = 6$ sessions). F indicates false goal zone and T indicates true goal zone. (*B*) Normalized probability of decoding actual position over the entire track for all cells (*Left*, purple circle), with a subset of place cells excluded (*center*, gray diamond), and with a subset of nonplace cells excluded (*Right*, black square). Regions inaccurately decoded as goal are highlighted in orange. Each line indicates one recording session; markers indicate mean, error bars indicate SEM. Asterisk indicates significant differences (paired *t* test, $q < 0.1$, FDR correction of six comparisons = 3 cell groups [all, excluding place cells, and excluding nonplace cells] × 2 genotypes). (*C*) Heat map of the differences between the decoded probability excluding a subset of place cells and including all cells (*Left*) and between the decoded probability excluding a subset of nonplace cells and including all cells, e.g., the difference between heatmaps shown in *A*. (*D*) As in *A* for decoding actual position relative to goal regardless of path ($n = 6$ sessions). (*E*) Normalized probability of decoding actual position relative to goal over the entire track for all cells (purple circle), with a subset of place cells excluded (gray diamond), and with a subset of nonplace cells excluded (black square). Each line indicates one recording session, markers indicate mean, and error bars indicate SEM. Asterisk indicates significant differences (paired-*t* test, $q < 0.1$, FDR correction of 150 comparisons = 6 whole track comparisons [3 cells group × 2 genotype] + 144 comparisons [18 positions × 3 cells group × 2 genotype over chance level, and cell type comparisons of 18 positions × 2 genotype]). (*F*) As in *C* for decoding along the path to reward regardless of path. Blue and red arrows indicate changes in the probability of decoding the true goal zone at the false goal zone when excluding place cells and nonplace cells, respectively. (*G*, *Top*) Normalized probability of decoding the goal zone along the whole path to the goal (purple). (*G*, *Bottom*) Difference between the decoded probability of decoding the goal zone when excluding a subset of place cells (gray diamonds) or a subset of nonplace cells (black square) compared to including all cells (purple line). Red asterisk indicates significantly higher than chance (one-sample *t* test, $q < 0.1$, FDR correction of 150 comparisons). Red arrowhead denotes less-strict statistics ($P < 0.05$, paired *t* test with no FDR correction). Black asterisk indicates significant cell type difference between excluding subsets of place cells versus nonplace cells (paired *t* test, $q < 0.1$, FDR correction of 150 comparisons).

the distance to goal, showing that both of these cell types contribute to distance to goal coding [Fig. 2 *E* and *F*; paired *t* test, q < 0.1 FDR correction of 150 comparisons; $P = 1.26e\text{-}4$, $F_{2,10}$ (cell type) = 25.116, one-way repeated measure ANOVA].

We then found that nonplace cell firing improved discrimination between the false (P3) and true (P6) goal zones compared to place cells. As described above, the false goal cue is identical to that in the true goal zone, but the true goal position is distinguishable based on the sequence of wall patterns and distal cues. We first noted higher decoding probability of positions with similar wall cues (located 90° from current position; Fig. 2*D*). Decoding of the true goal zone was significantly higher than chance levels when animals were at the false goal zone [Fig. 2*G*, *Top*; one-sample *t* test, q < 0.1, FDR correction of 150 comparisons; $P = 3.92e\text{-}14$, $F_{17,85}$ (location) = 10.196, one-way repeated measures ANOVA], thus producing ambiguous or mistaken decoding that is in conflict with the animal's current position. Not surprisingly, the decoding probability of the true goal zone was highest when the animal traversed the actual true goal zone, e.g., when the decoded position agreed with the current position (Fig. 2*G*, *Top*). Interestingly, excluding place and nonplace cells had different effects on decoding of the true goal zone at the false goal zone. Excluding place cells led to lower decoding probability of the true goal zone at the false goal zone (Fig. 2*G*, *Bottom*), meaning a reduction in mistaken decoding, showing that place firing contributed to poorer discrimination between the false and true goal zones (Fig. 2*G*, *Bottom*). In contrast, excluding nonplace cells led to a higher mistaken decoding probability of the true goal zone at the false goal zone [Fig. 2*G*, *Bottom*; $P = 0.010$, $t_5 = -4.069$, paired *t* test for cell type comparison at 80° to 90° spatial bin, q < 0.1, FDR correction of 150 comparisons; $P = 2.11e\text{-}9$, $F_{17,85}$ (location × cell type) = 6.412, two-way repeated measures ANOVA], meaning that nonplace cell firing improved discrimination between the false and true goal zones (Fig. 2 *F* and *G*). These decoding results were similar when excluding different percentages of cells (*SI Appendix*, Fig. S7). Together these results show that nonplace cells improve decoding of current position and distance to goal while also differentiating positions with similar cues but different task-relevance.

Nonplace Cell Firing Differs between Correct and Incorrect Performance. Having established that nonplace cells code task-relevant information, we then wondered if nonplace cell activity was modulated by task performance. If nonplace cell firing is important for task performance, we would expect this activity to differ on correct and incorrect trials. We hypothesized that if nonplace cells play a key role in coding distance to reward and distinguishing the false and true goal zones, they would fire differently at the false goal zone, and thus we focused on this area of the track (*SI Appendix*, Fig. S8 *A* and *B*). We identified trials when animals were engaged in the task based on routine licking behavior (see *SI Appendix*, *Supplementary Methods*) and defined correct and incorrect trials as trials where animals licked at least once or did not lick in the reward zone, respectively. We found no difference in overall firing rates of place cells as a function of position on correct and incorrect trials in no-reward zones, even at the false goal zone (*SI Appendix*, Fig. S8*B*; $P = 0.472$, $t_{195} = -0.721$, paired *t* test). In contrast, nonplace cells fired more at the false goal zone on correct than incorrect trials but not at other positions [*SI Appendix*, Fig. S8*B*; paired *t* test, q < 0.1 FDR correction of 24 comparisons; $P = 6.98e\text{-}5$, $F_{5,850}$ (location × performance) = 5.384, two-way repeated measures ANOVA]. Importantly, animals' speed was similar on correct and incorrect trials at the false goal zone (*SI Appendix*, Fig. S8*C*). Furthermore, we found significant spatial modulation of differences in firing rate of nonplace cells on correct and incorrect trials but no speed and lick modulation of these firing differences in a linear mixed effect model (linear mixed-effects [LME] model; see *SI Appendix*, *Statistics*) [$P = 0.005$, $F_{5,875.46}$ (location) = 3.363; $P = 0.597$, $F_{1,936.93}$ (speed) = 0.279; $P = 0.828$, $F_{1,1018.61}$ (lick) = 0.0470; LME model]. Therefore, differences in the firing of nonplace cells were likely not due to speed and licking behavior (*SI Appendix*, Fig. S8 *C* and *D*). These results show that the firing rates of nonplace cells are dependent on task performance.

We then tested the hypothesis that gamma modulation of nonplace cell firing is performance-dependent because gamma oscillations are thought to play a key role in spatial navigation. Thus, we examined whether gamma modulation of nonplace cell firing changes on correct and incorrect trials. We measured spike-field phase synchrony using pairwise phase consistency because this measure is less susceptible to differences in local field potential power, spike numbers, and trial numbers compared to classical methods such as phase locking values or spike-field coherence (52). These pairwise phase consistency values range from negative values for antiphasic modulation (with peaks greater than 90° apart) to 0 for no modulation (uniform distribution) to positive values for unimodal phasic modulation. Place cells showed no significant differences between correct and incorrect trials in their phase modulation as a function of position (Fig. 3 *A*–*C*; paired *t* test, q > 0.1, FDR correction for 480 comparisons). At the false goal zone, nonplace cells significantly differed in their modulation in the 20- to 40-Hz band, which overlapped with slow gamma (30 to 60 Hz), and trended differently for modulation in the 60- to 80-Hz band, which falls within medium gamma (60 to 100 Hz), between correct and incorrect trials [Fig. 3*C*; blue arrow, 20 to 40 Hz which overlapped with slow gamma: $P = 0.016$, $t_{61} = 2.485$, paired *t* test, q < 0.1, FDR correction for 480 comparisons; $P = 0.048$, $F_{5,305}$ (location × performance) = 2.270, two-way repeated measures ANOVA for 20 to 40 Hz; purple arrow, 60 to 80 Hz within M-gamma: $P = 0.064$, $t_{61} = -1.884$, $P = 0.061$, $F_{5,305}$ (location × performance) = 2.134, two-way repeated measures ANOVA for 60 to 80 Hz; $P = 2e\text{-}16$, $F_{9,549}$ (frequency) = 34.890, three-way repeated measure ANOVA]. Pairwise phase consistency (20 to 40 Hz) overlapped with slow gamma was significantly lower and negative on correct trials, indicating more antiphasic modulation. Pairwise phase consistency (60 to 80 Hz) within medium gamma trended more positive, indicating a trend of more unimodal phasic modulation. The differences in pairwise phase consistency of nonplace cells between correct and incorrect trials were not due to differences in gamma power at the false goal zone. We compared power across frequencies at the false goal zone on correct and incorrect trials and found no significant differences (*SI Appendix*, Fig. S9*B*, *Top*; unpaired *t* test; q > 0.1, FDR correction of 1,488 comparisons), although there was a small trend of increased medium gamma power on correct trials at false goal zone ($P = 0.032$, $t_{13} = -2.403$, at 66.41 Hz, paired *t* test; q > 0.1, FDR correction of 1,488 comparisons). Together, these results show that nonplace cells distinguish correct and incorrect trials in both their overall firing rates and in their spike timing modulation relative gamma oscillations.

Coinciding with performance-dependent changes in gamma modulation of nonplace cells, medium gamma occurrence increased and slow gamma occurrence decreased in the local field potential on correct trials. To identify the prevalence of

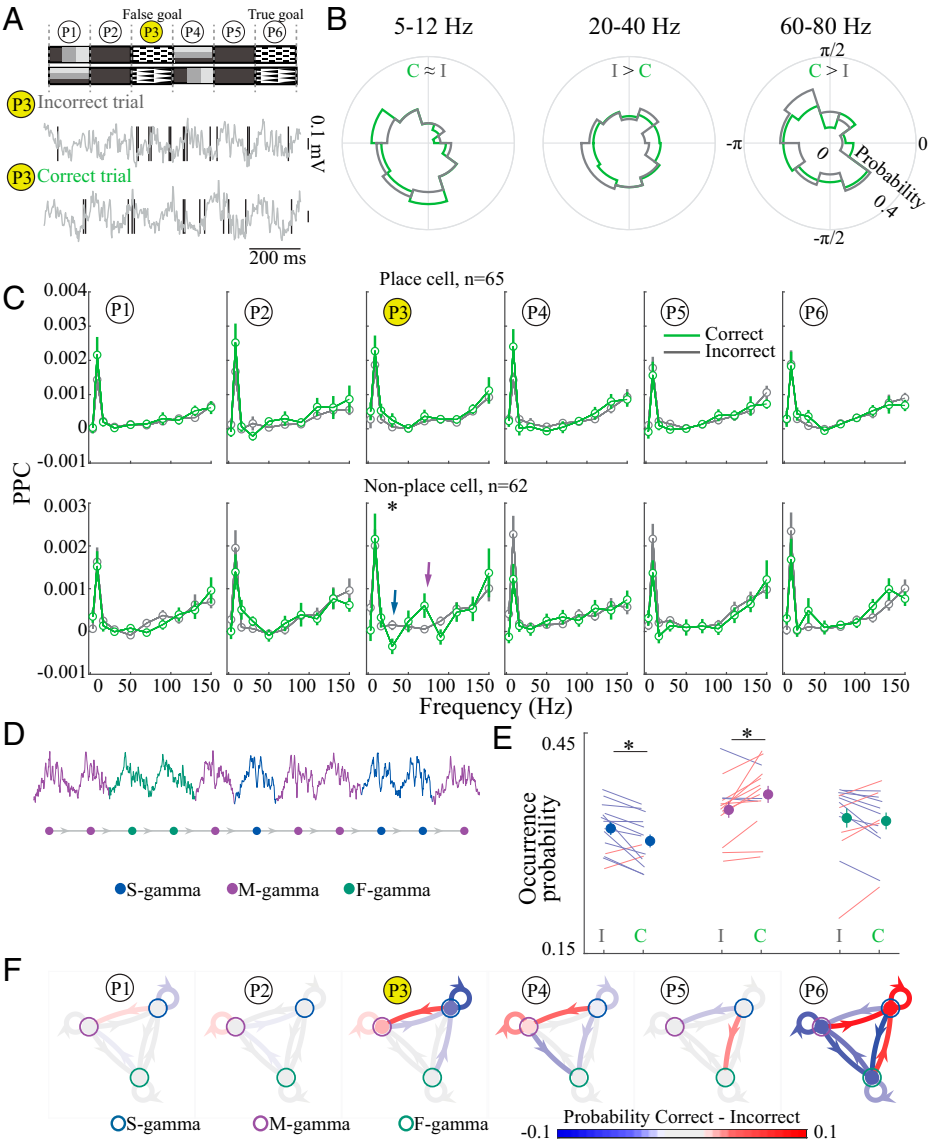

Fig. 3. Gamma modulation of nonplace cells differs on correct and incorrect trials. (*A*, *Top*) Schematic of cues in track with false goal zones at P3, yellow, with each half of the track shown as a separate row. (*A*, *Bottom*) Example LFP traces (gray line, mouse M8, Channel 17) and spikes (vertical line, unit 478) as an animal passes the false goal zone (P3 spatial bin) in one incorrect (*Left*) and correct (*Right*) trial. (*B*) Examples of spike-field phase synchrony measured using pairwise phase consistency (PPC) for spikes at the false goal zone for all incorrect trials (gray) and correct trials (green) relative to 5 to 12 Hz (theta band, *Left*), 20 to 40 Hz which overlapped with the slow gamma band (30 to 60 Hz, *Middle*), or 60 to 80 Hz within the medium gamma band (60 to 100 Hz, *Right*). (*C*) PPC of place cells (*Top*) and nonplace pyramidal cells (*Bottom*) for 10 frequency bands: delta (1 to 5 Hz), theta (5 to 12 Hz), beta (12 to 20 Hz), and nonoverlapping 20-Hz-wide frequency bands from 20 to 160 Hz across positions for all incorrect (gray) or correct (green) trials (mean ± SEM, $n = 65$ place cells, 62 nonplace pyramidal cells). Asterisk indicates significant differences between correct and incorrect trials (paired t test, q < 0.1, FDR correction from 480 comparisons, including paired comparisons for correct and incorrect trials and nonpaired comparisons between two genotypes over 10 frequency bands along six locations). The blue arrow indicates significant differences at 20 to 40 Hz ($P = 0.016$, $t_{61} = 2.485$, paired t test). The purple arrow indicates trending difference at 60 to 80 Hz ($P = 0.064$, $t_{61} = -1.884$, paired t test). (*D*) Examples local field potential trace identifying slow (blue), medium (purple), and fast (turquoise) gamma for one correct and incorrect trial. (*E*) Slow (*Left*), medium (*Middle*), and fast (*Right*) theta–gamma state occurrence over the track before the reward zone (P1 to P5) for incorrect and correct trials. Blue lines indicate decreasing and red lines indicate increasing occurrence on correct versus incorrect trials ($n = 14$ sessions after quality-control exclusion; see *SI Appendix, Supplementary Methods*). Asterisk denotes significant difference between correct trials and incorrect trials, FDR corrections for 48 comparisons (q < 0.1, 48 comparisons includes the comparisons between state occurrences, transitions, and two genotypes for correct or incorrect trials). (*F*) Summary of theta–gamma coupling state occurrences and transitions between correct and incorrect trials as a function of position. Red indicates higher probability and blue indicates lower probability on correct versus incorrect trials. Spatial bins as in *C*.

different types of gamma oscillations, we used a combination of signal processing and machine learning to identify gamma oscillations nested in theta for each theta cycle (Fig. 3*D* and *SI Appendix*, Fig. S10) (53). We found theta-nested medium gamma (60 to 100 Hz; *SI Appendix*, Fig. S10*F*, *Middle*), which is reported to arise from entorhinal inputs and sensory processing (28, 41, 54–56), was significantly more likely to occur on correct trials in nonreward zones [Fig. 3*E* and *SI Appendix*, Fig. S11 *A* and *C*; paired t test, q < 0.1, FDR correction for 48 comparisons; $P = 9.31\text{e-}6$, $F_{11,143}$ (theta-gamma transition type [TG-trans.] × performance) = 4.450, two-way repeated measures ANOVA]. Theta-nested slow gamma (30 to 60 Hz; *SI Appendix*, Fig. S10*F*, *Top*), which arises from CA3 (28, 41, 54–56), was significantly less likely to occur on correct trials in nonreward zones (Fig. 3*E* and *SI Appendix*, Fig. S11 *A* and *C*; paired t test, q < 0.1, FDR correction for 48 comparisons). When broken down by position, these differences were most prominent at the false goal zone (P3) and shortly thereafter

(P4) [Fig. 3*F* and *SI Appendix*, Fig. S11*E*; $P = 1.76e\text{-}8$, $F_{55,712}$ (TG-trans. × location) = 2.568, two-way repeated measures ANOVA]. Furthermore, we found more transitions from slow to medium gamma on correct trials in the same locations (Fig. 3*F* and *SI Appendix*, Fig. S11 *B, C,* and *F*). Theta–gamma coupling at the goal (P6) showed the opposite pattern: Slow gamma was more likely to occur while medium and fast gamma (100 to 160 Hz) were less likely to occur during each theta cycle (Fig. 3*F*). In sum, these findings show that slow gamma occurrence decreased and medium gamma increased in the face of ambiguous cue information preceding correct performance. Importantly, these changes in gamma occurrence coincided with gamma modulation of nonplace but not place cells on correct trials. Thus, these changes in the prevalence of different theta–gamma coupling oscillations preferentially modulated nonplace cells specifically at the false goal zone.

We then asked if differences in neural activity on correct versus incorrect trials could be explained by how long the animal has been performing the task. To control for these factors, we separately analyzed early versus late halves of the behavioral session, and we examined lick rate, speed, and neural activity in these two periods (*SI Appendix*, Fig. S12). In short, we found no significant differences in lick rate or speed at the false goal zone on early versus late trials (paired *t* test, q > 0.1, FDR correction of 22 comparisons). We also found no significant differences in GDI, pairwise phase consistency, or gamma occurrence on early versus late trials (*SI Appendix*, Fig. S12 *C–E*).

Deficits in Nonplace Cell Goal Discrimination and Gamma Modulation in a Mouse Model of AD. Finally, we asked how nonplace cell goal discrimination breaks down in a mouse model of AD with known learning impairments. By characterizing how nonplace cell goal discrimination changes when hippocampal function is impaired, we can better isolate aspects of nonplace activity that may be important versus incidental to hippocampal function. We determined how nonplace cell activity is altered in animals with spatial memory impairment and hippocampal pathology, specifically in the 5XFAD mouse model of AD, at an age when these mice have significant hippocampal synaptic loss and deficits in spatial memory (57, 58). 5XFAD mice were able to perform the same task as the WT littermates (*SI Appendix*, Fig. S13*A*), permitting comparisons between the two. Like WT mice, 5XFAD mice licked at the false goal zone more than other nonreward zones (*SI Appendix*, Fig. S13*B Top*; $P = 0.007$, $t_{18} = 3.024$ using paired *t* test, $P = 0.007$ using paired hierarchical bootstrap test; q < 0.1, FDR correction of 54 comparisons), but much less than at the true goal zone [$P = 1.74e\text{-}7$, $t_{18} = 8.195$ using paired *t* test, $P = 0$ using paired hierarchical bootstrap test; $P = 0$, $F_{2,68}$ (location) = 107.652; $P = 0.330$, $F_{1,34}$ (genotype) = 0.979; $P = 0.062$, $F_{2,68}$ (location × genotype) = 2.892; two-way mixed ANOVA for lick rate]. Interestingly, unlike WT mice, 5XFAD mice decreased their speed significantly more in the false goal zone compared to other zones [*SI Appendix*, Fig. S13*B Middle*; WT: $P = 0.114$, $t_{16} = -1.670$ using paired *t* test, $P = 0.246$ using paired hierarchical bootstrap test; 5XFAD: $P = 3.46e\text{-}5$, $t_{18} = -5.461$ using paired *t* test, $P = 0$ using paired hierarchical bootstrap test; q < 0.1, FDR correction of 54 comparisons; $P = 4.32e\text{-}4$, $F_{2,68}$ (location × genotype) = 8.702; two-way mixed ANOVA for speed] which could indicate poorer discrimination between the true and false goal zones.

In 5XFAD mice, place cells and nonplace cells exhibited both global position and goal distance coding (*SI Appendix*, Fig. S14 *A–C*). The GDI of nonplace cells trended more positive than that of place cells in 5XFAD mice, similar to WT mice [5XFAD: $P = 0.148$, $t_{421} = -1.450$, unpaired *t* test, WT: $P = 0.062$, $F_{1,741}$ (cell type) = 3.501; $P = 0.841$, $F_{1,741}$ (genotype) = 0.040; $P = 0.968$, $F_{1,741}$ (cell type × genotype) = 0.002; two-way ANOVA for all cells]. In contrast to WT mice, nonplace cells did not differ significantly from place cells when GDI was examined as a function of goal similarity or spatial information significance [*SI Appendix*, Fig. S14*D*; unpaired *t* test, q > 0.1, FDR correction for 20 comparisons, $P = 0.071$, $F_{1,741}$ (cell type × genotype) = 3.277; two-way ANOVA for goal similarity ≥ 0.1]. We then asked if GDI is correlated with task performance in 5XFAD and WT mice. We pooled cells from all animals together and observed a positive correlation between GDI and success rate in nonplace cells ($r = 0.173$, $P = 0.005$, Spearman's ρ test), indicating that animals with better goal discrimination performed better at the task (*SI Appendix*, Fig. S15). Importantly, no significant correlation was observed in place cells. Consistent with the findings above, excluding nonplace cells had no significant impact on decoding the goal zone when animals traversed nongoal zones in 5XFAD mice ($P > 0.05$ for each of the 150 comparisons, paired *t* test), and excluding nonplace cells did not differ significantly from excluding place cells (*SI Appendix*, Fig. S16). In line with our findings that 5XFAD mice decreased their speed at the false goals zones more than other nonreward zones, these results suggest that nonplace cells in 5XFAD mice did not discriminate between the true and false goals.

Prior research has shown deficits in place cell activity and in modulation of place cells by theta and gamma in other mouse models of AD (32, 59); however, nonplace cells have not been examined. We hypothesized that theta and gamma modulation of nonplace cells would also be altered in AD mice, specifically at the false goal zone in this task. First, we determined if 5XFAD mice had similar place or nonplace cell firing as that observed in WT littermates. We found both place cells and nonplace cells in 5XFAD mice. Place cells in 5XFAD mice had significantly lower spatial information than place cells in WT mice [*SI Appendix*, Fig. S17*A*; $P = 0.013$, Wilcoxon rank-sum test, q < 0.1, FDR correction of 25 comparisons; $P = 6.74e\text{-}12$, $F_{1,741}$ (cell type) = 48.663; $P = 0.717$, $F_{1,741}$ (genotype) = 0.131, $P = 0.736$, $F_{1,741}$ (cell type × genotype) = 0.114; two-way ANOVA]. Nonplace cells were not significantly different in 5XFAD and WT mice ($P = 0.095$, Wilcoxon rank-sum test), although this could be due to floor effects since spatial information was low in nonplace cells generally (*SI Appendix*, Fig. S17*A*). Furthermore, while firing rates of nonplace cells were higher on correct trials in WT mice at the false goal zone, no significant difference was found in 5XFAD mice (*SI Appendix*, Fig. S8*B*; paired *t* test, q > 0.1 FDR correction of 24 comparisons). In sum, we found that 5XFAD mice had deficits in spatial information in place cells and a lack of firing rate increases on correct trials in nonplace cells.

We then investigated gamma prevalence and performance-dependent gamma modulation in 5XFAD mice, because gamma is implicated in working memory and 5XFAD mice demonstrate memory deficits (57, 58). Again we focused on the false goal zone. First, we examined spiking modulation by theta oscillations because gamma oscillations in the hippocampus are nested in theta. In 5XFAD mice, spiking of place and nonplace cells was significantly less modulated by theta oscillations on correct trials [Fig. 4 *A* and *B*, *Left* and *SI Appendix*, Fig. S18; Paired *t* test, q < 0.1, FDR correction for 480 comparisons; $P = 8.68e\text{-}8$, $F_{1,182}$ (performance) = 31.117, two-way mixed ANOVA]. Second, modulation of nonplace cells spiking in the

20- to 40-Hz band (overlapped with slow gamma) or the 60- to 80-Hz band (within medium gamma) did not differ on correct or incorrect trials in 5XFAD mice, in contrast to what we found in WT mice [Figs. 3*C* and 4*B*, *Right* and *SI Appendix*, Fig. S18; $P = 0.040$, $F_{1,130}$ (genotype × performance) = 4.306 for 20 to 40 Hz, $P = 0.065$, $F_{1,130}$ (genotype × performance) = 3.475 for 60 to 80 Hz; two-way mixed ANOVA]. Instead, modulation of nonplace cell spiking in the 140- to 160-Hz band (within fast gamma) was significantly weaker on correct trials in 5XFAD mice compared to WT mice [Fig. 4*B*, *Right* and *SI Appendix*, Fig. S18; $P = 0.023$, $t_{130} = 2.296$, unpaired t test, q > 0.1, FDR correction for 480 comparisons; $P = 0.026$, $F_{1,130}$ (genotype) = 5.106, two-way mixed ANOVA for 140 to 160 Hz]. We found a general trend of decreased gamma power within the medium gamma band ($P < 0.1$, $t_{13} < -1.719$, for all frequencies between 60 and 72 Hz) and a trend of increased theta power around 8 Hz ($P = 0.024$, $t_{25} = -2.407$, unpaired t test) in 5XFAD mice. However, differences in gamma modulation of spiking between correct and incorrect trials in 5XFAD mice may not be explained by trending deficits in gamma power in these mice because genotype differences in LFP power occurred regardless of the animal's position or whether the trial was correct or incorrect (*SI Appendix*, Fig. S9*A*, blue arrows). At the false goal zone, we found no significant differences between gamma power on correct and incorrect trials in 5XFAD mice, similar to our findings in WT mice (*SI Appendix*, Fig. S9*B*, *Top*; paired t test, q > 0.1, FDR correction of 1,488 comparisons). Third, theta-nested medium gamma did not differ significantly on correct and incorrect trials in 5XFAD mice in contrast to WT mice (Fig. 4 *C–E* and *SI Appendix*, Fig. S11 *D–F*; $P = 0.069$, $t_{12} = -2.000$, paired t test). Performance-dependent changes in slow gamma occurrence were present in both 5XFAD and WT mice and theta-nested slow gamma was significantly less likely to occur on correct than incorrect trials in 5XFAD mice [Fig. 4 *C–E* and *SI Appendix*, Fig. S11 *E* and *F*; paired t test, q < 0.1 for 48 comparisons; $P = 1.19\text{e-}5$, $F_{1,25}$ (performance) = 29.641; $P = 0.080$, $F_{1,25}$ (genotype) = 3.331; $P = 0.548$, $F_{1,25}$

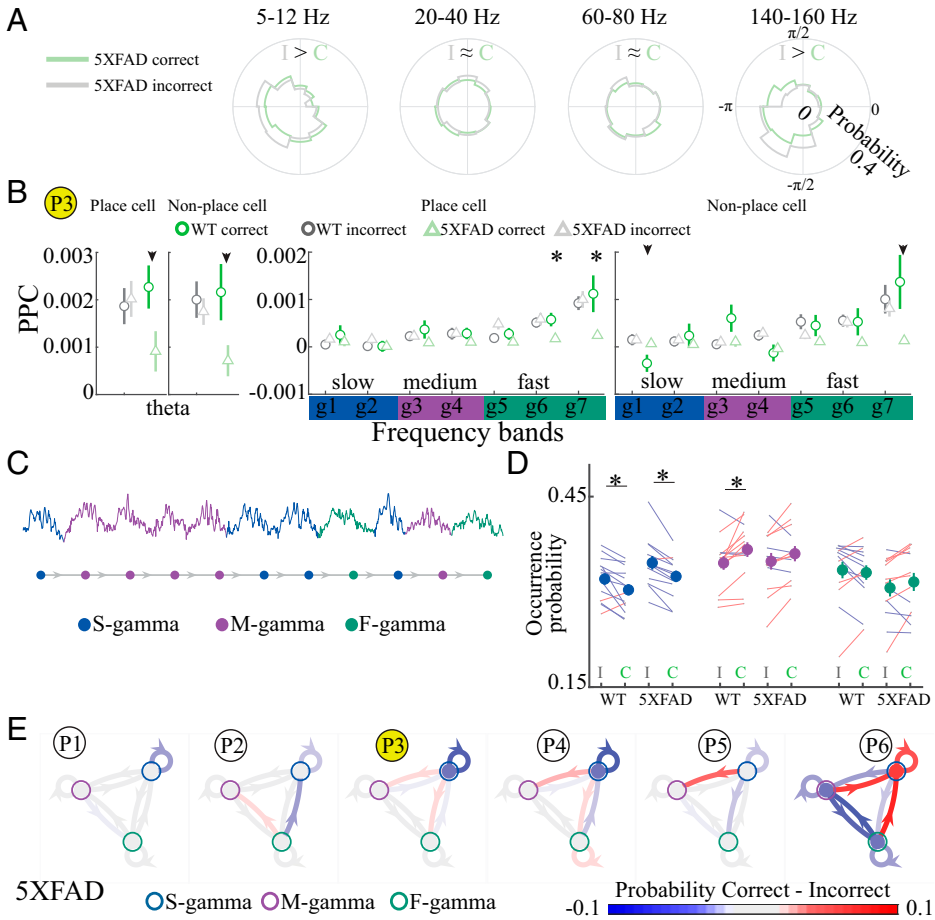

Fig. 4. Abnormal performance-dependent gamma modulation of nonplace cells in 5XFAD mice. (*A*) Examples of spike-field phase synchrony measured using pairwise phase consistency (PPC) for spikes at the false goal zone (P3) for all incorrect trials (gray) and correct trials (green) in 5XFAD mice relative to theta (*Left*), slow gamma (*Center Left*), medium gamma (*Center Right*), or fast gamma (*Right*). (*B*) PPC at the false goal zone of place cells (*Left*, $n = 65$, WT; $n = 114$, 5XFAD) and nonplace pyramidal cells (*Right*, $n = 62$, WT; $n = 70$, 5XFAD) for theta band (two left plots) and for slow (blue), medium (purple), and fast (turquoise) gamma bands (two right plots) for all incorrect (gray) or correct (green) trials for WT (circles) and 5XFAD (triangles) mice (mean ± SEM, g1: 20 to 40 Hz; g2: 40 to 60 Hz; g3: 60 to 80 Hz; g4: 80 to 100 Hz; g5: 100 to 120 Hz; g6: 120 to 140 Hz; g7:140 to 160 Hz). Asterisk indicates significant genotype differences (unpaired t test, q < 0.1, FDR correction from 480 comparisons including nonpaired comparisons between two genotypes and paired comparisons for correct and incorrect trials); black arrowhead denotes less-strict statistics ($P < 0.05$, paired t test with no FDR correction). (*C*) Examples local field potential trace identifying slow (blue), medium (purple), and fast (turquoise) gamma for one correct and incorrect trial. (*D*) Slow (*Left*), medium (*Middle*), and fast (*Right*) theta–gamma state occurrence over the track before the reward zone (P1 to P5) for incorrect and correct trials before entering reward zones. Blue lines indicate decreasing and red lines indicate increasing occurrence on correct versus incorrect trials. Asterisk denotes significant difference (paired t test for performance comparisons and unpaired t test for genotype comparisons; q < 0.1, FDR corrections for 48 comparisons includes the comparisons of state occurrences, transitions, and two genotypes for correct or incorrect trials; $n = 14$, WT; $n = 13$, 5XFAD sessions). (*E*) Theta–gamma state occurrence and transition difference between correct and incorrect trials across positions for 5XFAD animals ($n = 13$ sessions).

(performance × genotype) = 0.372; two-way mixed ANOVA]. In sum, we find that 5XFAD mice have a lack of performance-dependent changes in firing rates of nonplace cells, gamma modulation of nonplace cells, and medium gamma occurrence.

Discussion

We examined nonplace cell activity at multiple levels while mice performed a spatial navigation task in which spatial cues provide ambiguous information about the goal. At the single-cell level, nonplace cell firing discriminated between true and false goals. At a population level, both place cells and nonplace cells represented current positions and distance to goals, but only nonplace cell firing improved accurate decoding of the false versus true goal. Furthermore, at the false goal cue, nonplace cell firing differed on correct and incorrect trials with higher firing, stronger negative slow gamma phase modulation, and a trend of more positive medium gamma-phase modulation on correct trials while place cells showed no such differences. These results indicate nonplace cells play a key role as goal-discriminating cells, and this coding is amplified by gamma modulation. Importantly, these results are not due to environmental sampling, speed, or licking behavior as these did not differ between correct and incorrect trials. Finally, we found deficits in this goal-discriminating activity in nonplace cells in animals with memory impairment and hippocampal dysfunction, the 5XFAD mouse model of AD.

Neuroscientists have long studied cells that fire depending on specific external features such as place cells tuned to an animal's position (4, 5) or visual cells tuned to the orientation of a visual stimulus (60). However, many neurons are not clearly tuned to a particular feature of external stimuli and remained understudied. Recent work reveals that these seemingly "untuned" neurons also contributed to coding external information at the population level in multiple brain circuits (26, 27, 60–66). Within this study, we aim to elucidate the role of cells that, at the single-cell level, do not have significant spatial information or clear spatial receptive fields during goal-directed spatial navigation. We show that hippocampal nonplace cells not only contribute to spatial coding, they play a different role than place cells. Our work reveals that nonplace cells code for nonplace task-relevant features like information about goals. This goal information cannot be readily encoded by place cells without weakening their place codes. Thus, these findings provide a fundamental insight that "untuned" cells carry valuable behaviorally relevant information that "tuned" cells cannot. Furthermore, because many standard methods assume cells are tuned to a stimulus, our work highlights ways to identify these "untuned" contributions to coding, via task design, discrimination analysis, population decoding of conflicting positions, and gamma modulation. We treated place and nonplace cells as separate groups to study their respective contributions; however, the question remains whether place and nonplace cells are categorically different. Nonplace cells did not reach criteria of significant spatial information; however, they could be part of a continuum of spatial coding in hippocampus (26, 27). Broadly, these findings point to a need to examine coding contribution of nonplace cells in the hippocampus and the specific roles of "untuned" cells in multiple circuits.

Prior work has not investigated hippocampal coding for goal-related information when spatial cues are ambiguous about goals. While prior work has investigated goal coding in place cells, such coding seems to vary depending on the task. Several studies have shown that place fields cluster around rewarded locations (14, 16). There are conflicting reports about whether CA1 place cells encode reward location or additional reward information such as reward values (67–69). One study found place cells remapped around new goal locations only if goals were not marked by a visual cue that indicates reward (15). Another line of research has shown that when animals receive a reward, place cell reactivation increases during sharp wave ripples, high-frequency oscillations with corresponding bursts of population activity that are essential for learning and memory (70, 71). These prior studies typically examined place cells, not nonplace cells. We find that nonplace cells discriminate between ambiguous cues for true and false goals. Thus, nonplace cells and task-relevant coding may become more obvious and more relevant when place information is unreliable or ambiguous.

While prior work has shown nonplace cells contribute to spatial coding, we find that these cells play a role in discriminating similar spatial cues and their activity differs between correct and incorrect performance (26, 27). Gamma modulation of nonplace cell firing distinguishes between correct and incorrect trials, showing that gamma may amplify some codes over others. Gamma oscillations are thought to amplify some signals over others by driving neurons to fire together in short time windows, which in turn is more likely to drive downstream regions (72, 73). Indeed, gamma modulation enhances signal transmission and sensory inputs that arrive as specific phases of gamma oscillations are more likely to generate spiking responses (74, 75). The observed spiking modulation of nonplace cells may be further amplified by increased medium gamma and decreased slow gamma occurrence on correct trials. Because slow gamma has been shown to indicate stronger CA3–CA1 coupling and medium gamma stronger EC–CA1 coupling (28, 41, 54–56), these results could indicate a shift to a greater influence of entorhinal and sensory inputs and a smaller influence of CA3 inputs and recall. Place cell firing during slow gamma has been shown to more strongly represent nonlocal positions during recall, while such firing during medium gamma has been shown to more strongly represent current position (29, 35). Importantly, the changes we observed in spiking modulation and medium and slow gamma occurrence primarily transpired at the false goal zone. At the false goal, the sequence of prior sensory cues is more informative about the appropriate behavioral response (run versus slow down and lick) than simple cue–reward associations involving the current sensory cue. Thus, medium gamma carrying such sensory information may be especially important at the false goal zone, in line with observed increases in medium gamma and decreases in slow gamma at the false goal zone. Indeed, excessive slow gamma can be maladaptive: Slow gamma has been shown to predominate in mice that are inflexible when learning new places to avoid and tend to recall old avoided locations (29). However, important questions remain about what levels of gamma modulation are physiologically relevant. Finally, our results show abnormal theta–gamma oscillations and spike timing relative to these oscillations in a mouse model of AD. Unlike WT mice, 5XFAD mice decreased their speed significantly more in the false goal zone compared to other zones, which could indicate poorer discrimination between the true and false goal zones. These results underline the importance of spike timing in task performance and disease.

An important consideration is whether these place and nonplace cells we have identified generalize beyond our task. Prior work has established some differences between place cells in VR and real-world exploration. For example, in VR place cells

tend to be more likely to code distance along a track and have lower peak firing rates, and a lower proportion of recorded pyramidal cells have significant place coding than in real-world exploration (25). There are, nevertheless, similarities between VR and real-world spatial coding; place cells in VR have significant spatial information and clear place fields (76). It has also been suggested that nonhuman primate hippocampal coding is perhaps more similar to coding observed in rodent VR versus real-world tasks (77). Importantly, we find that place cells in our task contribute to decoding of current position, in line with many prior studies in both real-world and VR recordings (47, 49, 78, 79). Furthermore, other studies using real-world tasks have shown that nonplace cell firing contributed to place coding (26). We also show nonplace cells contributed to place coding in line with these prior studies. Thus, while there may be some differences, both place and nonplace cells have clear similarities between the real world and VR.

In sum, we find that nonplace cells carry task-relevant information about goals when spatial information is ambiguous, and this type of coding fails in a mouse model of AD. We deem these cells to be goal-discriminating cells. Gamma modulation of the firing activity of these goal-discriminating, nonplace cells distinguishes between correct and incorrect trials. These findings add further support to theories that gamma oscillations amplify some codes over others, and these results point to the need to consider information carried by nonplace cells and other cells without clear coding schemes.

Materials and Methods

In total 14 male mice (11 to 14 mo old) were involved in this study, including six WT and eight 5XFAD mice on a C57BL/6 background. Neural recordings in CA1 were performed using a 32-channel, single-shank probe (NeuroNexus) during a VR task while animals ran on a spherical treadmill. See *SI Appendix, Supplementary Methods* for details of surgical procedures, behavioral training, electrophysiology recordings, and data analysis. Biological replicates were defined as electrodes, experimental sessions, neurons, or animals as indicated in different analyses.

All animal work was approved by the National Institutes of Health guidelines on animal care and use at Georgia Institute of Technology.

Data Availability. The datasets and code to generate the figures in the current study are available on GitHub (https://github.com/singerlabgt/NonPlaceCell/) (80).

ACKNOWLEDGMENTS. A.C.S. acknowledges the Packard Foundation and NIH-NINDS R01 NS109226. S.M.P. was supported by NSF GRFP Grants DGE-1444932 and T32NS096050-22. A.L.P. was supported by NIH NRSA 5F31AG066410. We thank Dr. Joseph Manns and members of the A.C.S. laboratory for feedback on the methods, results, and manuscript and Dr. Jiyuan Hu from New York University for comments on linear mixed-effect models analysis.

1. C. Meneghetti, E. Labate, E. Toffalini, F. Pazzaglia, Successful navigation: The influence of task goals and working memory. *Psychol. Res.* **85**, 634–648 (2021).
2. H. Eichenbaum, The role of the hippocampus in navigation is memory. *J. Neurophysiol.* **117**, 1785–1796 (2017).
3. G. Buzsáki, E. I. Moser, Memory, navigation and theta rhythm in the hippocampal-entorhinal system. *Nat. Neurosci.* **16**, 130–138 (2013).
4. J. O'keefe, L. Nadel, *The Hippocampus as a Cognitive Map* (Oxford University Press, 1978).
5. J. O'Keefe, Place units in the hippocampus of the freely moving rat. *Exp. Neurol.* **51**, 78–109 (1976).
6. N. Burgess, J. O'Keefe, Neuronal computations underlying the firing of place cells and their role in navigation. *Hippocampus* **6**, 749–762 (1996).
7. E. J. Markus *et al.*, Interactions between location and task affect the spatial and directional firing of hippocampal neurons. *J. Neurosci.* **15**, 7079–7094 (1995).
8. J. Lisman *et al.*, Viewpoints: How the hippocampus contributes to memory, navigation and cognition. *Nat. Neurosci.* **20**, 1434–1447 (2017).
9. B. Poucet *et al.*, Spatial navigation and hippocampal place cell firing: The problem of goal encoding. *Rev. Neurosci.* **15**, 89–107 (2004).
10. T. Kobayashi, A. H. Tran, H. Nishijo, T. Ono, G. Matsumoto, Contribution of hippocampal place cell activity to learning and formation of goal-directed navigation in rats. *Neuroscience* **117**, 1025–1035 (2003).
11. M. Wang, D. J. Foster, B. E. Pfeiffer, Alternating sequences of future and past behavior encoded within hippocampal theta oscillations. *Science* **370**, 247–250 (2020).
12. L. M. Frank, E. N. Brown, M. Wilson, Trajectory encoding in the hippocampus and entorhinal cortex. *Neuron* **27**, 169–178 (2000).
13. H. T. Ito, S. J. Zhang, M. P. Witter, E. I. Moser, M. B. Moser, A prefrontal-thalamo-hippocampal circuit for goal-directed spatial navigation. *Nature* **522**, 50–55 (2015).
14. L. Zinyuk, S. Kubik, Y. Kaminsky, A. A. Fenton, J. Bures, Understanding hippocampal activity by using purposeful behavior: Place navigation induces place cell discharge in both task-relevant and task-irrelevant spatial reference frames. *Proc. Natl. Acad. Sci. U.S.A.* **97**, 3771–3776 (2000).
15. D. Dupret, J. O'Neill, B. Pleydell-Bouverie, J. Csicsvari, The reorganization and reactivation of hippocampal maps predict spatial memory performance. *Nat. Neurosci.* **13**, 995–1002 (2010).
16. V. Hok *et al.*, Goal-related activity in hippocampal place cells. *J. Neurosci.* **27**, 472–482 (2007).
17. J. L. Gauthier, D. W. Tank, A dedicated population for reward coding in the hippocampus. *Neuron* **99**, 179–193.e7 (2018).
18. Z. Xiao, K. Lin, J.-M. Fellous, Conjunctive reward–place coding properties of dorsal distal CA1 hippocampus cells. *Biol. Cybern.* **114**, 285–301 (2020).
19. H. J. Spiers, C. Barry, Neural systems supporting navigation. *Curr. Opin. Behav. Sci.* **1**, 47–55 (2015).
20. W. E. Skaggs, B. L. McNaughton, Spatial firing properties of hippocampal CA1 populations in an environment containing two visually identical regions. *J. Neurosci.* **18**, 8455–8466 (1998).
21. B. Poucet, V. Hok, Remembering goal locations. *Curr. Opin. Behav. Sci.* **17**, 51–56 (2017).
22. R. W. Komorowski, J. R. Manns, H. Eichenbaum, Robust conjunctive item-place coding by hippocampal neurons parallels learning what happens where. *J. Neurosci.* **29**, 9918–9929 (2009).
23. J. J. Moore, J. D. Cushman, L. Acharya, M. R. Mehta, Hippocampal representations of distance, space, and direction and their plasticity predict navigational performance. *bioRxiv* [Preprint] (2021). https://www.biorxiv.org/content/10.1101/2020.12.30.424858v1 (Accessed 28 February 2021).
24. H. J. Spiers, H. F. Olafsdottir, C. Lever, Hippocampal CA1 activity correlated with the distance to the goal and navigation performance. *Hippocampus* **28**, 644–658 (2018).
25. Z. M. Aghajan *et al.*, Impaired spatial selectivity and intact phase precession in two-dimensional virtual reality. *Nat. Neurosci.* **18**, 121–128 (2015).
26. F. Stefanini *et al.*, A distributed neural code in the dentate gyrus and in CA1. *Neuron* **107**, 703–716.e4 (2020).
27. L. Meshulam, J. L. Gauthier, C. D. Brody, D. W. Tank, W. Bialek, Collective behavior of place and non-place neurons in the hippocampal network. *Neuron* **96**, 1178–1191.e4 (2017).
28. J. Yamamoto, J. Suh, D. Takeuchi, S. Tonegawa, Successful execution of working memory linked to synchronized high-frequency gamma oscillations. *Cell* **157**, 845–857 (2014).
29. D. Dvorak, B. Radwan, F. T. Sparks, Z. N. Talbot, A. A. Fenton, Control of recollection by slow gamma dominating mid-frequency gamma in hippocampus CA1. *PLoS Biol.* **16**, e2003354 (2018).
30. P. R. Shirvalkar, P. R. Rapp, M. L. Shapiro, Bidirectional changes to hippocampal theta-gamma comodulation predict memory for recent spatial episodes. *Proc. Natl. Acad. Sci. U.S.A.* **107**, 7054–7059 (2010).
31. J. B. Trimper, C. R. Galloway, A. C. Jones, K. Mandi, J. R. Manns, Gamma oscillations in rat hippocampal subregions dentate gyrus, CA3, CA1, and subiculum underlie associative memory encoding. *Cell Rep.* **21**, 2419–2432 (2017).
32. A. J. Mably, B. J. Gereke, D. T. Jones, L. L. Colgin, Impairments in spatial representations and rhythmic coordination of place cells in the 3xTg mouse model of Alzheimer's disease. *Hippocampus* **27**, 378–392 (2017).
33. L. L. Colgin, E. I. Moser, Gamma oscillations in the hippocampus. *Physiology (Bethesda)* **25**, 319–329 (2010).
34. G. Buzsaki, *Rhythms of the Brain* (Oxford University Press, 2006).
35. K. W. Bieri, K. N. Bobbitt, L. L. Colgin, Slow and fast γ rhythms coordinate different spatial coding modes in hippocampal place cells. *Neuron* **82**, 670–681 (2014).
36. G. Buzsáki *et al.*, Hippocampal network patterns of activity in the mouse. *Neuroscience* **116**, 201–211 (2003).
37. A. Bragin *et al.*, Gamma (40-100 Hz) oscillation in the hippocampus of the behaving rat. *J. Neurosci.* **15**, 47–60 (1995).
38. J. Csicsvari, B. Jamieson, K. D. Wise, G. Buzsáki, Mechanisms of gamma oscillations in the hippocampus of the behaving rat. *Neuron* **37**, 311–322 (2003).
39. A. Ylinen *et al.*, Sharp wave-associated high-frequency oscillation (200 Hz) in the intact hippocampus: Network and intracellular mechanisms. *J. Neurosci.* **15**, 30–46 (1995).
40. L. L. Colgin, Rhythms of the hippocampal network. *Nat. Rev. Neurosci.* **17**, 239–249 (2016).
41. E. W. Schomburg *et al.*, Theta phase segregation of input-specific gamma patterns in entorhinal-hippocampal networks. *Neuron* **84**, 470–485 (2014).
42. J. J. Tukker, P. Fuentealba, K. Hartwich, P. Somogyi, T. Klausberger, Cell type-specific tuning of hippocampal interneuron firing during gamma oscillations in vivo. *J. Neurosci.* **27**, 8184–8189 (2007).
43. D. Dvorak, A. Chung, E. H. Park, A. A. Fenton, Dentate spikes and external control of hippocampal function. *Cell Rep.* **36**, 109497 (2021).
44. P. Ravassard *et al.*, Multisensory control of hippocampal spatiotemporal selectivity. *Science* **340**, 1342–1346 (2013).
45. P. D. Rich, H. P. Liaw, A. K. Lee, Large environments reveal the statistical structure governing hippocampal representations. *Science* **345**, 814–817 (2014).
46. A. C. Singer, M. P. Karlsson, A. R. Nathe, M. F. Carr, L. M. Frank, Experience-dependent development of coordinated hippocampal spatial activity representing the similarity of related locations. *J. Neurosci.* **30**, 11586–11604 (2010).
47. E. N. Brown, L. M. Frank, D. Tang, M. C. Quirk, M. A. Wilson, A statistical paradigm for neural spike train decoding applied to position prediction from ensemble firing patterns of rat hippocampal place cells. *J. Neurosci.* **18**, 7411–7425 (1998).
48. M. P. Karlsson, L. M. Frank, Awake replay of remote experiences in the hippocampus. *Nat. Neurosci.* **12**, 913–918 (2009).
49. T. J. Davidson, F. Kloosterman, M. A. Wilson, Hippocampal replay of extended experience. *Neuron* **63**, 497–507 (2009).

50. A. B. Saleem, E. M. Diamanti, J. Fournier, K. D. Harris, M. Carandini, Coherent encoding of subjective spatial position in visual cortex and hippocampus. *Nature* **562**, 124–127 (2018).
51. M. F. Carr, S. P. Jadhav, L. M. Frank, Hippocampal replay in the awake state: A potential substrate for memory consolidation and retrieval. *Nat. Neurosci.* **14**, 147–153 (2011).
52. M. Vinck, F. P. Battaglia, T. Womelsdorf, C. Pennartz, Improved measures of phase-coupling between spikes and the Local Field Potential. *J. Comput. Neurosci.* **33**, 53–75 (2012).
53. L. Zhang, J. Lee, C. Rozell, A. C. Singer, Sub-second dynamics of theta-gamma coupling in hippocampal CA1. *eLife* **8**, e44320 (2019).
54. L. L. Colgin *et al.*, Frequency of gamma oscillations routes flow of information in the hippocampus. *Nature* **462**, 353–357 (2009).
55. B. Lasztóczi, T. Klausberger, Hippocampal place cells couple to three different gamma oscillations during place field traversal. *Neuron* **91**, 34–40 (2016).
56. V. J. López-Madrona *et al.*, Different theta frameworks coexist in the rat hippocampus and are coordinated during memory-guided and novelty tasks. *eLife* **9**, 1–35 (2020).
57. Y. Buskila, S. E. Crowe, G. C. R. Ellis-Davies, Synaptic deficits in layer 5 neurons precede overt structural decay in 5xFAD mice. *Neuroscience* **254**, 152–159 (2013).
58. H. Oakley *et al.*, Intraneuronal beta-amyloid aggregates, neurodegeneration, and neuron loss in transgenic mice with five familial Alzheimer's disease mutations: Potential factors in amyloid plaque formation. *J. Neurosci.* **26**, 10129–10140 (2006).
59. F. Cacucci, M. Yi, T. J. Wills, P. Chapman, J. O'Keefe, Place cell firing correlates with memory deficits and amyloid plaque burden in Tg2576 Alzheimer mouse model. *Proc. Natl. Acad. Sci. U.S.A.* **105**, 7863–7868 (2008).
60. D. H. Hubel, T. N. Wiesel, Receptive fields of single neurones in the cat's striate cortex. *J. Physiol.* **148**, 574–591 (1959).
61. M. L. Leavitt, F. Pieper, A. J. Sachs, J. C. Martinez-Trujillo, Correlated variability modifies working memory fidelity in primate prefrontal neuronal ensembles. *Proc. Natl. Acad. Sci. U.S.A.* **114**, E2494–E2503 (2017).
62. A. Ponce-Alvarez, A. Thiele, T. D. Albright, G. R. Stoner, G. Deco, Stimulus-dependent variability and noise correlations in cortical MT neurons. *Proc. Natl. Acad. Sci. U.S.A.* **110**, 13162–13167 (2013).
63. Y. Chen, W. S. Geisler, E. Seidemann, Optimal decoding of correlated neural population responses in the primate visual cortex. *Nat. Neurosci.* **9**, 1412–1420 (2006).
64. A. B. A. Graf, A. Kohn, M. Jazayeri, J. A. Movshon, Decoding the activity of neuronal populations in macaque primary visual cortex. *Nat. Neurosci.* **14**, 239–245 (2011).
65. J. Zylberberg, J. Cafaro, M. H. Turner, E. Shea-Brown, F. Rieke, Direction-selective circuits shape noise to ensure a precise population code. *Neuron* **89**, 369–383 (2016).
66. M. Levy, O. Sporns, J. N. MacLean, Network analysis of murine cortical dynamics implicates untuned neurons in visual stimulus coding. *Cell Rep.* **31**, 107483 (2020).
67. H. Lee, J. W. Ghim, H. Kim, D. Lee, M. Jung, Hippocampal neural correlates for values of experienced events. *J. Neurosci.* **32**, 15053–15065 (2012).
68. O. Mamad *et al.*, Place field assembly distribution encodes preferred locations. *PLoS Biol.* **15**, e2002365 (2017).
69. É. Duvelle *et al.*, Insensitivity of place cells to the value of spatial goals in a two-choice flexible navigation task. *J. Neurosci.* **39**, 2522–2541 (2019).
70. A. C. Singer, L. M. Frank, Rewarded outcomes enhance reactivation of experience in the hippocampus. *Neuron* **64**, 910–921 (2009).
71. C. G. McNamara, Á. Tejero-Cantero, S. Trouche, N. Campo-Urriza, D. Dupret, Dopaminergic neurons promote hippocampal reactivation and spatial memory persistence. *Nat. Neurosci.* **17**, 1658–1660 (2014).
72. G. Buzsáki, X. J. Wang, Mechanisms of gamma oscillations. *Annu. Rev. Neurosci.* **35**, 203–225 (2012).
73. W. Singer, C. M. Gray, Visual feature integration and the temporal correlation hypothesis. *Annu. Rev. Neurosci.* **18**, 555–586 (1995).
74. J. A. Cardin *et al.*, Driving fast-spiking cells induces gamma rhythm and controls sensory responses. *Nature* **459**, 663–667 (2009).
75. V. S. Sohal, F. Zhang, O. Yizhar, K. Deisseroth, Parvalbumin neurons and gamma rhythms enhance cortical circuit performance. *Nature* **459**, 698–702 (2009).
76. G. Chen, J. A. King, N. Burgess, J. O'Keefe, How vision and movement combine in the hippocampal place code. *Proc. Natl. Acad. Sci. U.S.A.* **110**, 378–383 (2013).
77. S. Wirth, P. Baraduc, A. Planté, S. Pinède, J.-R. Duhamel, Gaze-informed, task-situated representation of space in primate hippocampus during virtual navigation. *PLoS Biol.* **15**, e2001045 (2017).
78. D. Aronov, D. W. Tank, Engagement of neural circuits underlying 2D spatial navigation in a rodent virtual reality system. *Neuron* **84**, 442–456 (2014).
79. R. Bourboulou *et al.*, Dynamic control of hippocampal spatial coding resolution by local visual cues. *eLife* **8**, e44487 (2019).
80. L. Zhang, S. M. Prince, A. L. Paulson, A. C. Singer, Non-place cell data. GitHub. https://github.com/singerlabgt/NonPlaceCell/. Deposited 1 December 2021.